Preprint typeset in JHEP style. - HYPER VERSION

arXiv:1005.xxxx
May 21, 2010

Spin Discrimination in Three-Body Decays

Lisa Edelhäuser[1,a], **Werner Porod**[1,2,b], **Ritesh K. Singh**[1,c]

[1] *Institut für Theoretische Physik und Astrophysik, Universität Würzburg, D-97074 Würzburg, GERMANY*

[2] *AHEP Group, Instituto de Física Corpuscular – C.S.I.C./Universitat de València*
E–46071 València, Spain

Email: [a] ledelhaeuser@physik.uni-wuerzburg.de,
[b] porod@physik.uni-wuerzburg.de,
[c] singh@physik.uni-wuerzburg.de

Abstract: The identification of the correct model for physics beyond the Standard Model requires the determination of the spin of new particles. We investigate to which extent the spin of a new particle X can be identified in scenarios where it decays dominantly in three-body decays $X \to f\overline{f}Y$. Here we assume that Y is a candidate for dark matter and escapes direct detection at a high energy collider such as the LHC. We show that in the case that all intermediate particles are heavy, one can get information on the spins of X and Y at the LHC by exploiting the invariant mass distribution of the two standard model fermions. We develop a model-independent strategy to determine the spins without prior knowledge of the unknown couplings and test it in a series of Monte Carlo studies.

Keywords: Spin determination, model discrimination.

Contents

1. Introduction

With the start of the Large Hadron Collider (LHC) the direct exploration of physics at the TeV scale has begun. The hunt for new physics is one of the major topics in the experimental program of the LHC. Many of these models predict partners of the known standard model (SM) particles, which usually have the same quantum numbers and properties but for the mass and the spin assignment. For example, in

supersymmetric (SUSY) models the fermions have scalar partners whereas in models with universal extra dimensions (UED) fermionic partners are predicted. Due to the astrophysical requirement of explaining the dark matter (DM) relic density of the universe, these models usually invoke an additional discrete symmetry leading to a new stable particle which in general escapes detection at future collider experiments. Examples are R-parity in SUSY models or Kaluza-Klein-parity in UED where e.g. the lightest neutralino or the lightest Kaluza-Klein (KK) excitation of the vector bosons is the corresponding DM candidate, respectively. The generic signature at LHC are in both cases SM-fermions with high transverse momentum and missing energy stemming from the escaping DM candidate.

An important question is: How can one distinguish between different models? These models differ in the spins of the predicted new particles and, thus, one has to develop methods to get information on the spin. First attempts have been made for s-channel resonances [1, 2, 3, 4] and in case of subsequent two-body decays of the new particles [5, 6, 7, 8, 9, 10, 11, 12, 13, 14, 15, 16, 17] where in many cases model dependent assumptions had been made. An additional possibility to get information on the spin is cross section measurements provided one knows the representation of the particle produced [18], e.g. whether it is a colour triplet or a colour octet. Hardly any attempt has been made so far in case of three-body decays but for the case of distinguishing a gluino from the KK excitation of a gluon [19] and the quantum interference method [20, 21, 22, 23] which, in principle, is also valid for three-body decays. The quantum interference method requires fully reconstructed events which can be achieved at the ILC and only in few processes at the LHC. In contrast, our method in this paper does not require full reconstruction of events. In this paper we start a series of investigations on how one can extract information on the spins of new particles in a model independent way if three-body decays are dominating.

We concentrate here on the case of the direct production of a new particle X decaying via a three-body decay into two SM-fermions and a new invisible particle Y, which escapes detection. We will show that the invariant mass distribution of the two detectable fermions contains sufficient information to extract the spins of the unknown particles in such a decay.

In this paper, we consider cases where the intermediate particles are very heavy compared to the decaying one. Examples of such cases are e.g. split SUSY with very heavy scalars [24], split UED [25] or higgsless supersymmetric models [26]. As it turns out, in this limit it is possible to determine the spin of the decaying particle and the invisible particle provided the masses of the new particles are known to some extent. In contrast to model dependent approaches to spin determination [19, 27], we follow a bottom-up approach that can be used for all models with heavy intermediate particles and only renormalizable operators. The case of lighter intermediate particles will be presented in a subsequent paper.

This paper is organised as follows: We first present the basic ideas using a toy

model in section 2. Afterwards, we present a convenient parametrisation of the differential width for the three-body decays as the product of a phase space factor and a polynomial. In section 3 we develop a strategy to determine the spins exploiting specific properties of the coefficients of this polynomial. We also investigate the impact of different decay topologies and discuss qualitatively the influence of the mass of the intermediate particle. In section 4 we test our strategy with the help of Monte Carlo examples and conclude in section 5. The formulas of the various coefficients are given in the appendix.

2. Basic Idea and General Setting

We investigate decays of the type $X \to f\bar{f}Y$ where X and Y are new particles being either scalars, vector bosons or fermions. Here we assume that all 2-body decays of X are either kinematically forbidden or at least loop-suppressed compared to the tree-level three-body decays considered. As mentioned above we assume that all off-shell particles, which we denote collectively by I, mediating these decays are much heavier than X, e.g. $m_I \gg m_X$. In practice it is sufficient to assume $m_I \gtrsim 5m_X$ as we will show below. In addition we assume that Y is a colour singlet as it should serve as potential dark matter candidate.

We will be as general as possible by taking the most generic Lagrangian with arbitrary couplings of $\mathcal{O}(1)$ and dimension 4 operators. From this we calculate the widths for the decays of Y assigning different spins to X and Y, respectively. To simplify the notation we will abbreviate the decays $S \to f\bar{f}S$, $S \to f\bar{f}V$, $V \to f\bar{f}S$, $V \to f\bar{f}V$ and $F \to f\bar{f}F$ by (S,S), (S,V), (V,S), (V,V) and (F,F), where S, V and F stand for scalar, vector boson and fermion, respectively. Note, that the fermionic case covers both, Dirac- and Majorana-fermions.

After integrating over the momentum of the escaping particle Y, we expand the differential widths in powers of $\epsilon = m_X/m_I$ and give the resulting expressions as a phase space factor times a Laurent series (actually polynomials in most cases) of a dimensionless quantity $\hat{s}$ which is derived from the invariant mass $s = (p_f + p_{\bar{f}})^2$, p_f and $p_{\bar{f}}$ are the four momenta of the SM-fermions. Note, that $s = m^2_{f\bar{f}}$ in the case of subsequent two body decays studied in the literature [5, 6, 7, 8, 9, 16, 17, 28].

Most of the features can be understood by considering the decays of a particle X charged under $SU(3)$ into two massless quarks and Y . Considering coloured particles in the first place is motivated by the fact that they in general have sizable cross sections at the LHC. Moreover, due to gauge invariance only a subset of all topologies are allowed which simplifies the obtained expressions considerably. Therefore we will first discuss these cases. The additional features of either taking X as an $SU(3)$ singlet and/or the case that the SM-fermions being massive (i.e. top quarks) will be discussed afterwards.

The coefficients in the Laurent series depend obviously on the couplings and masses of the particles involved and one might ask if and how one gets information on the spins without knowing these quantities. It turns out we have to assume in our approach that the mass of Y and the mass difference $(m_X - m_Y)$ are known within a given uncertainty but in general we do not need any information on the underlying couplings. The basic idea is that different spin assignments lead to different relations between these coefficients which can be exploited. There is however one obstacle: one cannot exclude on logical grounds that there is a 'conspiracy' between the couplings suppressing the dominant terms in the ϵ expansion. This complicates life somewhat but even in that case relations between the coefficients are maintained as discussed below.

2.1 Dependence of the invariant mass distribution on the spins of unknown particles

We first discuss a set of toy models where the new particles X and Y are either scalars and/or vector bosons coupling to massless u-quarks and an additional heavy fermion which we assume to be a Majorana-fermion. The invariant fermion mass squared is $s = (p_f + p_{\bar{f}})^2 = E_1 E_2 \cdot (1 - \cos\theta_{f\bar{f}})$ where E_i are the SM fermion energies and $\theta_{f\bar{f}}$ is the angle between them in the rest-frame of X. In Figure 1 we show the differential decay width divided by the phase space factor which is shown independently (red/full line). The behaviour of the different curves can be understood using helicity and spin arguments.

The SM-fermions have definite helicity states as we have assumed them to be massless. There are two kinematical configurations where the spatial angular momentum in the rest-frame of X is zero corresponding to $\cos\theta_{f\bar{f}} = \pm 1$: (i) The particle Y is at rest and the two fermions are back to back corresponding to $\cos\theta_{f\bar{f}} = -1$ with $s = s_{max}$. In this case the total spin of the fermions sums up to one if it is either an $u_L\bar{u}_L$ or $u_R\bar{u}_R$ combination whereas the total spin of the fermions is zero for the $u_L\bar{u}_R$ and $u_R\bar{u}_L$ combinations. Here we have introduced $u_{L,R} = P_{L,R}\, u$ with $P_{L,R} = (1 \mp \gamma_5)/2$. (ii) The particle Y flies opposite to the two fermions which are flying parallel now corresponding to $\cos\theta_{f\bar{f}} = 1$ with $s_{min} = 0$. In this case the total spin of the fermions sums up to one if it is either a $u_L\bar{u}_R$ or a $u_R\bar{u}_L$ combination whereas the total spin of the fermions is zero for the $u_L\bar{u}_L$ and $u_R\bar{u}_R$ combinations.

(S, S)**:**

The matrix element M_{fi} for this decay has the generic form

$$M_{fi} = \overline{u}_u\ (g_r P_R + g_l P_L) S_I (n_l^* P_R + n_r^* P_L) v_u \simeq \frac{1}{m_I} \overline{u}_u (g_r n_l^* P_R + g_l n_r^* P_L) v_u$$

corresponding to the $u_L\bar{u}_R$ and $u_R\bar{u}_L$ combinations since in the limit of a very heavy intermediate particle the corresponding propagator reduces to $S_I = 1/(\not{p} - m_I) \simeq$

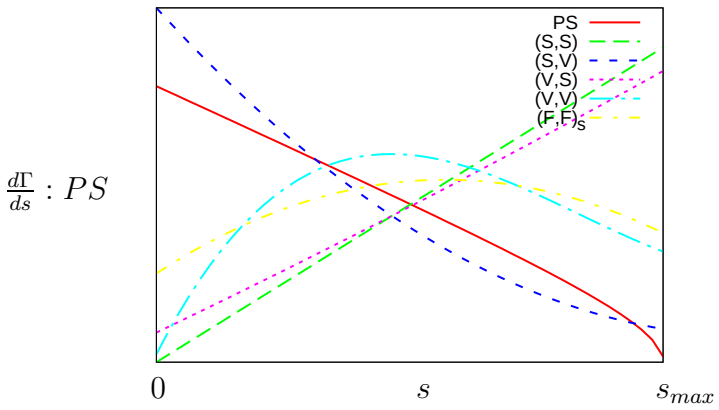

Figure 1: Differential width divided by a phase space factor PS for the different decays $X \to f\overline{f}Y$, $X, Y \in S, V$ taking $m_f = 0$, $m_X/m_Y = 0.1$ and all couplings equal. In addition the phase space factor is drawn.

$1/m_I$. As the total angular momentum of the final state has to be zero, the matrix element has to vanish in case $\cos\theta_{f\bar{f}} = 1$ ($s = 0$) as can also be seen in Fig. 1 whereas for $\cos\theta_{f\bar{f}} = -1$ the helicity assignment yields a non-vanishing matrix element. In the plot we have taken for all cases $n_l = n_r = g_l = g_r$.

(S, V)**:**

This process has a more involved structure since the vector boson can have polarisation $\pm 1, 0$. Using the matrix element one sees that in contrast to the previous case one expects a non-vanishing matrix element for all s

$$\begin{aligned} M_{fi} &= \overline{u}_u \ (g_r P_R + g_l P_L) S_I \gamma_\mu (n_l^* P_R + n_r^* P_L) v_u \epsilon_Y^\mu \\ &\simeq \frac{1}{m_I} \overline{u}_u \gamma_\mu (g_r n_r^* P_L + g_l n_l^* P_R) v_u \epsilon_Y^\mu . \end{aligned}$$

These are the $u_L \bar{u}_L$ and $u_R \bar{u}_R$ combinations where for $s = 0$ the total spin of the fermions is zero and for $s = s_{max}$ it is one. In the limit $\theta_{f\overline{f}} \to 0$ ($s \to 0$) the amplitude is proportional to $((m_X/m_Y)^2 - 1)$ $(m_X^2 - m_Y^2)$. The first factor is larger and diverges as $m_Y \to 0$ which reflects the longitudinal component of the vector boson. This can be nicely seen in the blue (dashed) line in Fig. 1.

(V, S)**:**

In this case, we start with a spin 1 boson. A similar reasoning as before shows that the general trend should be opposite to the $S \to f\bar{f}V$ case which is confirmed by Fig. 1 (pink/small dashed line).

(V, V)**:**

This decay can have several helicity combinations which we want to sketch here. The matrix reads

$$M_{fi} = \overline{u}_u \ \gamma_\mu (g_r P_R + g_l P_L) S_I \gamma_\nu (n_r^* P_L + n_l^* P_R) v_u \epsilon_Y^\nu \epsilon_X^{\mu *}$$

$$\simeq \frac{1}{m_I}\overline{u}_u\ \gamma_\mu\gamma_\nu(g_r n_r^* P_L + g_l n_l^* P_l)v_u\epsilon_Y^\nu\epsilon_X^{\mu*}$$

As in the (S,S) case we find the $u_L\bar{u}_R$ and $u_R\bar{u}_L$ combinations. However, now in principle for all s one can expect a non-vanishing matrix element squared. However, as can be seen in Fig. 1 it can be zero for $s = 0$ for special combinations of the couplings, e.g. as in our case with $n_l = n_r = g_l = g_r$ (cyan/dot-dashed line). In this sense the example shown is an extreme case and in general the matrix element will be non-zero for $s = 0$.

2.2 General structure of the differential widths

We now discuss the general structure for the decays

$$X(p, m_X) \to f(q_1, m_f) + \overline{f}(q_2, m_f) + Y(q_3, m_Y) \tag{2.1}$$

with X and Y being scalars (S), vectors (V) or fermions (F) and heavy intermediate particles I with mass m_I. We will consider several contributions at the same time and assume that the masses of all intermediate particles are equal to maximise interference effects which usually complicate things. Beside the usual Mandelstam variables

$$\begin{aligned} s = (p-q_3)^2 = (q_1+q_2)^2\ ;\ t = (p-q_2)^2 = (q_1+q_3)^2 \\ \text{and}\ \ u = (p-q_1)^2 = (q_2+q_3)^2 = -s-t-m_X^2-m_Y^2+2m_f^2 \end{aligned}$$

we introduce the dimensionless parameters τ_i and $\hat{s}$

$$\hat{s} = \frac{\left(4\tau_f^2 + (\tau_Y-1)^2\right) - \frac{2s}{m_X^2}}{\left(4\tau_f^2 - (\tau_Y-1)^2\right)}\ ;\ \tau_Y = \frac{m_Y}{m_X}\ ;\ \tau_f = \frac{m_f}{m_X}\ ;\ \tau_C = \frac{M_C}{m_X} \tag{2.2}$$

where M_C denotes dimensionful couplings, e.g. as they appear in the ZZH vertex or the trilinear soft SUSY breaking parameters A_i. We note that $\hat{s}_{min} = -1$ and $\hat{s}_{max} = 1$.

We expand the matrix elements squared in powers of $\epsilon = m_X/m_I$ and perform an integration over t as in this way we integrate over the momentum of the unobserved particle Y. For the t-integration we find the boundaries

$$\begin{aligned} t_\pm = \frac{1}{4}m_X^2\Bigg(&(\tau_Y+1)^2 + \hat{s}\left(4\tau_f^2 - (\tau_Y-1)^2\right) \\ &\pm \left((\tau_Y-1)^2 - 4\tau_f^2\right) \times \sqrt{\frac{(1-\hat{s}^2)\left((1-\hat{s})((\tau_Y-1)^2-4\tau_f^2)+8\tau_Y\right)}{4\tau_f^2+(\tau_Y-1)^2+\hat{s}\left((\tau_Y-1)^2-4\tau_f^2\right)}}\Bigg) \end{aligned} \tag{2.3}$$

$$PS = \int_{t_-}^{t_+} dt$$

$$= \left((\tau_Y-1)^2-4\tau_f^2\right)\frac{m_X^2}{2}\sqrt{\frac{(1-\hat{s}^2)\left((1-\hat{s})((\tau_Y-1)^2-4\tau_f^2)+8\tau_Y\right)}{4\tau_f^2+(\tau_Y-1)^2+\hat{s}\left((\tau_Y-1)^2-4\tau_f^2\right)}} \quad (2.4)$$

where we have also defined the 'phase space' PS. In this way the differential decay rate can be written as

$$\frac{d\Gamma}{d\hat{s}} = \frac{PS}{(2\pi)^3\ 256\ m_X}\left(\frac{Z}{(a\hat{s}+b)^2}+\frac{A}{a\hat{s}+b}+B+C\cdot\hat{s}+D\cdot\hat{s}^2+E\cdot\hat{s}^3+F\cdot\hat{s}^4\right) \quad (2.5)$$

where $a=\left((\tau_Y-1)^2-4\tau_f^2\right)$ and $b=\left((\tau_Y-1)^2+4\tau_f^2\right)$. The prefactors $Z,A,\ldots,F$ are functions of ϵ, the τ_i and the couplings. Note that Z and F only appear in the case of the decay (V,V). As we exemplify the main features for massless SM-fermions, we display Eq. (2.4) for this case:

$$\begin{aligned} t_\pm &= \tfrac{1}{4}m_X^2\left((\tau_Y+1)^2-\hat{s}(\tau_Y-1)^2\pm(1-\tau_Y)\sqrt{(1-\hat{s})\left((1-\hat{s})(\tau_Y-1)^2+8\tau_Y\right)}\right)\\ \mathrm{PS} &= \tfrac{1}{2}m_X^2(1-\tau_Y)\sqrt{(1-\hat{s})\left((1-\hat{s})(\tau_Y-1)^2+8\tau_Y\right)} \end{aligned} \quad (2.6)$$

2.2.1 Decays of bosons

As one can see from Table 1, there are three 'topologies' which contribute differently to the decay rate. The second 'topology' only contributes if both, the Y- and the X-particle, are their own anti-particles. Obviously, topologies 1 and 2 will in general contribute at $\mathcal{O}(\epsilon^2)$ whereas the third one in general only at $\mathcal{O}(\epsilon^4)$ due to the different structures of the propagators. Only in the case where the dimensionfull scalar-vector-vector or triple scalar couplings are of $\mathcal{O}(m_I)$, the third topology might contribute at a smaller power of ϵ as will be discussed below. In the further calculation we neglect terms higher than $\mathcal{O}(\epsilon^4)$.

The generic Lagrangian density for these decays reads as

$$\mathcal{L}_{i,j,k} = X_i\overline{I}_f\widetilde{G}_i f + Y_i\overline{I}_f\widetilde{N}_i f + I_i\overline{f}\widetilde{T}_i f + I_i X_j Y_k\widetilde{\Gamma}_{ijk} + h.c. \quad (2.7)$$

where $i,j,k = s,v$ and I_i is the intermediate off-shell particle. The generic couplings are given by

$$\begin{aligned} &\widetilde{G}_i: G_s = (g(r,s)P_R+g(l,s)P_L)\,;\ G_v = \gamma^\mu\left(g(r,v)P_R+g(l,v)P_L\right)\\ &\widetilde{N}_i: N_s = (n(r,s)P_R+n(l,s)P_L)\,;\ N_v = \gamma^\mu\left(n(r,v)P_R+n(l,v)P_L\right)\\ &\widetilde{T}_i:\ T_s = (s(r)P_R+s(l)P_L)\,;\qquad T_v = \gamma^\mu\left(v(r)P_R+v(l)P_L\right) \end{aligned} \quad (2.8)$$

and for $\widetilde{\Gamma}_{ijk}$

$$\begin{aligned} &\Gamma_{sss} = c(s)M_C; && \Gamma_{vvs}=\Gamma_{vsv}=\Gamma(v^\mu,v^\nu,s)=c(v)M_C g^{\mu\nu}\\ &\Gamma_{svv}=\Gamma(s,v^\mu,v^\nu)=c(s)M_C g^{\mu\nu}; && \Gamma_{vs_1s_2}=\Gamma(v^\mu,s_1,s_2)=c(v)(p_{s_2}-p_{s_1})^\mu\\ &\Gamma_{s_1s_2v}=\Gamma_{s_1vs_2}=\Gamma(s_1,s_2,v^\mu)=c(s)(p_{s_2}-p_{s_1})^\mu\\ &\Gamma_{v_1v_2v_3}=\Gamma(v_1^\nu,v_2^\rho,v_3^\mu)=c(v)((p_{v_1}-p_{v_2})^\mu g^{\nu\rho}+(p_{v_2}-p_{v_3})^\nu g^{\mu\rho}+(p_{v_3}-p_{v_1})^\rho g^{\mu\nu}) \end{aligned} \quad (2.9)$$

Decay	Top. 1	Top. 2	Top. 3(s/v)	
(S,S)	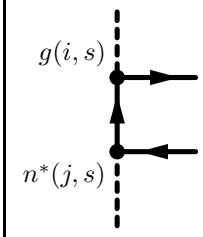	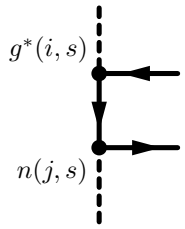	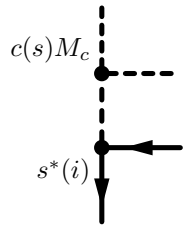	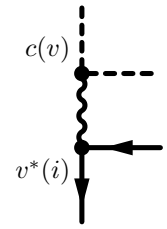
(S,V)	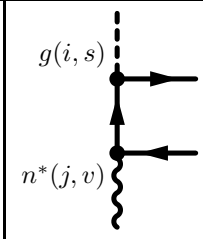	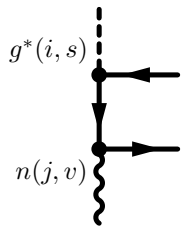	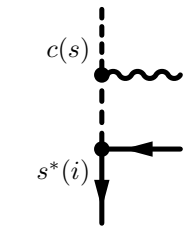	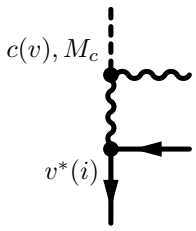
(V,S)	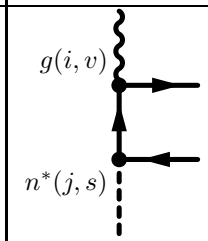	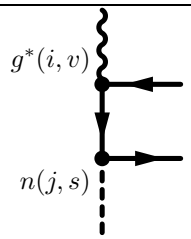	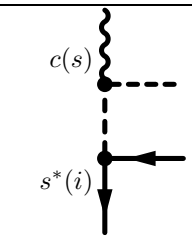	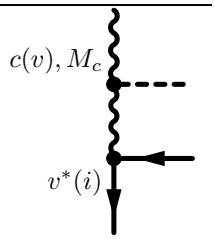
(V,V)	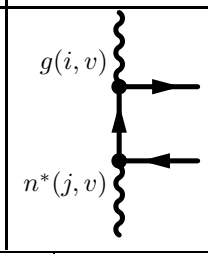	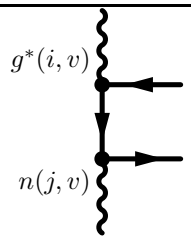	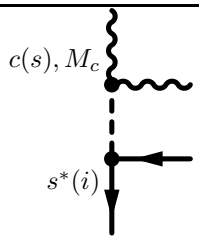	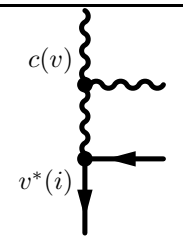

Top. 1 (s)	Top. 2 (s)	Top. 3 (s)	Top. 1 (v)	Top. 2 (v)	Top. 3 (v)
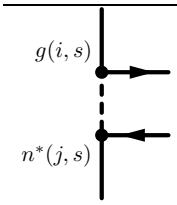	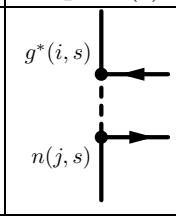	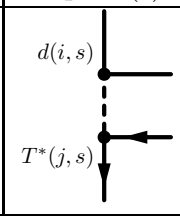	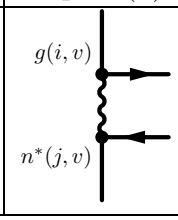	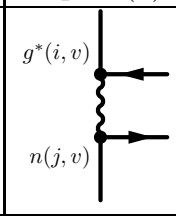	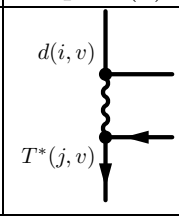

Table 1: Topologies for the decays of bosons $X \to f\overline{f}Y$ (top) and fermions (F,F) (bottom) with $i,j \in \{l,r\}$ (see also Eq. (2.8)).

where the indices of the vertex expressions Γ_{ijk} correspond to those of the Lagrangian in Eq. 2.8.

The matrix element including all topologies shown in Table 1 reads

$$\begin{aligned}\mathcal{M}_{i,j} = \quad & \overline{u}(q_1, m_f) G_i \not{F}_p \ \gamma^0 N_j^\dagger \gamma^0 \ v(q_2, m_f) \epsilon_i(p) \epsilon_j(q_3) \\ & + \overline{u}(q_1, m_f) N_j \not{F}_p \ \gamma^0 G_i^\dagger \gamma^0 \ v(q_2, m_f) \epsilon_i(p) \epsilon_j(q_3) \\ & + \sum_{k=s,v} \Gamma_{kij} W_{P,i} \overline{u}(q_1, m_f) \gamma^0 T_k^\dagger \gamma^0 v(q_2, m_f)\end{aligned} \tag{2.10}$$

with the 'polarisation' vectors

$$\epsilon_s = \mathbb{1}; \quad \epsilon_v = \widetilde{\epsilon}^\mu$$

and the fermion and boson propagators

$$F_p = i\frac{\not{p} + m_I}{p^2 - m_I^2}; \quad W_{P,s} = i\frac{1}{p^2 - m_I^2}; \quad W_{P,v} = -i\frac{\left(g^{\mu\nu} - p^\mu p^\nu / m_I^2\right)}{p^2 - m_I^2} \tag{2.11}$$

2.2.2 Decays of fermions

In this case the generic Lagrangian is given by

$$\mathcal{L}_i = I_i \overline{f} G_i M_x + I_i \overline{f} N_i M_y + I_i \overline{M_y} \Gamma_i M_x + I_i \overline{f} T_i f + h.c. \tag{2.12}$$

where $M_{x,y}$ denote the spinors of the new fermions and $i = s, v$ denotes whether the exchanged particle is a scalar or a vector boson. The couplings are similar to those above:

$$\begin{aligned}\mathcal{M}_i = \quad & \Big[\overline{u}(q_1, m_f) G_i u(p, m_X)\Big] \ W_{p,i} \ \Big[\overline{u}(q_3, m_Y) \gamma^0 N_i^\dagger \gamma^0 v(q_2, m_f)\Big] \\ & + \Big[\overline{u}(q_1, m_f) N_i v(q_3, m_Y)\Big] \ W_{p,i} \ \Big[\overline{v}(p, m_X) \gamma^0 G_i^\dagger \gamma^0 v(q_2, m_f)\Big] \\ & + \Big[\overline{u}(q_3, m_Y) \Gamma_i u(p, m_X)\Big] \ W_{p,i} \ \Big[\overline{u}(q_1, m_f) \gamma^0 T_i^\dagger \gamma^0 v(q_2, m_f)\Big]\end{aligned} \tag{2.13}$$

corresponding to the topologies given in Table 1 with the same couplings as in Eq. (2.8, 2.9) and additionally:

$$\begin{aligned} & i = s: \ \Gamma_s = (d(s, r) P_R + d(s, l) P_L) \\ & i = v: \ \Gamma_v = \gamma^\mu \left(d(v, r) P_R + d(v, l) P_L\right)\end{aligned} \tag{2.14}$$

3. Strategy for Spin Identification

In this section we discuss the strategy for discriminating the various scenarios with different spins assigned to the particles X and Y. The procedure is to find suitable relations or to mark the signs of the different coefficients $Z, A, \ldots, F$. This is done in the second part of this chapter. Before this we will have a look at the different topologies and their contribution depending on the chosen colour structure.

Our main focus here is on the case of massless fermions as this is already sufficient to get the required information. This immediately implies a considerable simplification because some of the coefficients for the differential width are zero and we obtain

$$\frac{d\Gamma}{d\hat{s}} = \frac{PS}{(2\pi)^3\ 256\ m_X}\left(B + C\hat{s} + D\hat{s}^2 + E\hat{s}^3 + F\hat{s}^4\right) \tag{3.1}$$

The formulas for the coefficients are given in the appendix for the corresponding lowest order in ϵ. For the case (S,S) we also give the higher orders up to ϵ^4. Moreover, it turns out that the decays in top-quarks, the only SM fermion with mass of $\mathcal{O}(100\text{ GeV})$, behave in the same way and the discrimination is also possible in this case as will be discussed at the end of this section. This implies that one has a second system to test the spin assignments in an independent way.
We start with a subset of the topologies given in Table 1, namely topologies 1 and 2 as these are typically realised in extensions of the SM, e.g. in models with extra dimensions or in SUSY. Moreover, we will first further restrict ourselves to scenarios where X is charged under $SU(3)$, e.g. a colour octet gluino or a KK excitation of a gluon, and Y is electrically neutral and uncharged under $SU(3)$. This is motivated by the fact that the LHC is a hadron collider. In the second step we add the third topology. But it turns out that in the case of scalar contributions to (S,S) and (S,V) gauge invariance allows only two additional terms because the SM-fermions are charged under $SU(3)$. However, these contributions will in general be of order ϵ^4 due to the boson propagator except for the case where the trilinear scalar coupling is of order m_I in which there might be contributions at order $\mathcal{O}(\epsilon^2)$. In the third step we will also discuss the complications and their potential solutions in case that X is an $SU(3)$ singlet.

3.1 Signs of the coefficients

It turns out that some of the coefficients have a definite sign independent of the couplings and masses involved. This important fact will be used later to discriminate between the different spin assignments of X and Y. We collected the signs of the different coefficients for all decays of bosons in Table 2 where we have expanded the coefficients in powers of ϵ, e.g.

$$B = \sum_{k=2}^{4} B_k \epsilon^k \tag{3.2}$$

Some of the signs in Table 2 are obtained analytically but several are gained numerically by scanning and inserting random couplings in the range $[-1,1]$. There are some coefficients where the sign cannot be determined without knowing the mass ratios or the couplings which are marked by "$\pm$". Moreover, we have put a 0 whenever the coefficient itself vanishes. We give the signs for three cases, ordered from the most general one to the most restricted one: (i) X is an $SU(3)$ singlet, where

	(S,S)			(S,V)		(V,S)		(V,V)	
ϵ^2	s	c	1+2	s	c/1+2	s	c/1+2	s	c/1+2
B_2	+	+	+	+	+	+	+	±	±
C_2	+	+	+	±	±	+	+	±	±
D_2	0	0	0	+	+	+	+	±	±
E_2	0	0	0	0	0	0	0	+	+
ϵ^3									
B_3	±	±	0	±	0	±	0	±	0
C_3	±	±	0	±	0	±	0	±	0
D_3	0	0	0	±	0	±	0	±	0
E_3	0	0	0	0	0	0	0	±	0
ϵ^4									
B_4	+	+	+	+	+	+	+	+	+
C_4	±	+	+	±	±	±	±	±	±
D_4	±	−	−	±	±	±	±	±	±
E_4	0	0	0	±	±	±	±	±	±
F_4	0	0	0	0	0	0	0	±	±

Table 2: Signs of the coefficients for the case of a boson decaying into another boson and massless SM-fermions in the final state for different powers of ϵ. The rows correspond to the cases: (s) X is an $SU(3)$ singlet, (c) X is charged under $SU(3)$ taking all possible topologies into account and $(1+2)$ X is charged under $SU(3)$ taking topologies 1+2 into account. The ± marks the cases where the sign cannot be determined without knowing the masses/couplings and 0 marks the cases with a vanishing coefficient.

all topologies of Table 1 contribute. The corresponding columns are denoted by s. (ii) X is charged under $SU(3)$ and all possible contributions allowed are taken into account and the corresponding columns are denoted by c. (iii) X is charged under $SU(3)$ and only topologies 1+2 contribute and, thus, the corresponding columns are denoted by 1+2. In the subsequent sections these cases will be discussed in the reversed order focussing on the terms of order ϵ^2. The ϵ^4 order is only of interest, if the leading order is zero, which is the case for some special coupling arrangements discussed in section 3.4.

In case of a new fermion X it turns out that the result does neither depend on the spin of the exchanged particle nor on the topology, e.g. it does not matter if all topologies are taken or only a subset. Since we have only bosonic propagators there are only the $\mathcal{O}(\epsilon^4)$ contributions and we find:

$$\text{sign}(B_4) = + \quad , \quad \text{sign}(C_4) = \pm \quad , \quad \text{sign}(D_4) = - \quad , \quad \text{sign}(E_4) = 0 \tag{3.3}$$

3.2 Decays into massless SM-fermions in case of topologies 1+2

Let's assume that we have measured the differential decay width of a new particle

and determined the coefficients introduced above accurately in a fit. In section 4 we will discuss first Monte Carlo studies at the parton level where we also review the obtainable accuracy. This can be combined with our knowledge on the various coefficients introduced so far to determine the spins of the new particles or at least to exclude certain possibilities. The main strategy is summarised in Fig. 2 and explained in some more detail below.

Let's start with the E term which is only non-zero in the (V,V) case. This immediately implies that (V,V) is preferred once the 'measured' E term is larger than 0. For consistency we check that $B > 0$. The next step is to look at the D term as for $D \neq 0$ and $E = 0$ the sign of D determines whether one is dealing with fermions ($D < 0$) or bosons ($D \geq 0$) where the latter case includes (S,S), (S,V) and (V,S). In case of $D = 0$ only the case (S,S) remains. To further distinguish the cases (S,V) and (V,S) from each other, one has to consider the ratios:

$$\begin{array}{ll}
(S,V):\ D/C = \frac{(\tau_Y-1)^2}{22\tau_Y^2-4\tau_Y-2} & \in [-\infty,-\frac{1}{3}]\cup[0,\infty] \\
(V,S):\ D/C = -\frac{(\tau_Y-1)^2}{2(\tau_Y(\tau_Y+2)-11)} & \in [0,\frac{1}{22}] \\
(S,V):\ C/B = \frac{22\tau_Y^2-4\tau_Y-2}{\tau_Y(25\tau_Y+6)+1} & \in [-2,\frac{1}{2}] \\
(V,S):\ C/B = \frac{8(\tau_Y+9)}{\tau_Y(\tau_Y+6)+25}-2 & \in [\frac{1}{2},\frac{22}{25}] \\
(S,V):\ D/B = \frac{(\tau_Y-1)^2}{\tau_Y(25\tau_Y+6)+1} & \in [0,1] \\
(V,S):\ D/B = \frac{(\tau_Y-1)^2}{\tau_Y(\tau_Y+6)+25} & \in [0,\frac{1}{25}]
\end{array} \tag{3.4}$$

since here the dependence on the unknown couplings cancel as can be seen from eqs. (A.6) and (A.7). For these decays we have three possible ratios shown in Eq. (3.4). We see that the ratio C/B has no overlap and hence best suited ratio to distinguish between (S,V) and (V,S). The D/B and D/C ratios seem to be less useful since the intervals overlap, but except for $\tau_Y = 1$, e.g. $m_Y = m_X$, but they are never equal for $\tau_Y \neq 1$. In the range where τ_Y is close to one, the SM-fermions become very soft and this part will be excluded because a lower cut on their energies is put in practice. Last but not least we note that the (S,S) can be further checked by the requirement that $B/C = 1$ as can be seen from Eq. (A.3). Therefore, independent of the mass ratios, one can state that all those five cases can be discriminated from each other.

3.3 Impact of the third topology

We have seen in section 2.2 that the dominant contributions stem from topologies 1 and 2 of Table 1 in case of decays of bosons because the third topology generally contributes at $\mathcal{O}(\epsilon^4)$. One might asked if one of the dimensionful couplings in the diagrams of the third topology can become so large to disturb the above strategy. Note, that in case of a new fermions higher orders in ϵ have no impact and, thus, we restrict the discussion here to decays of bosons.

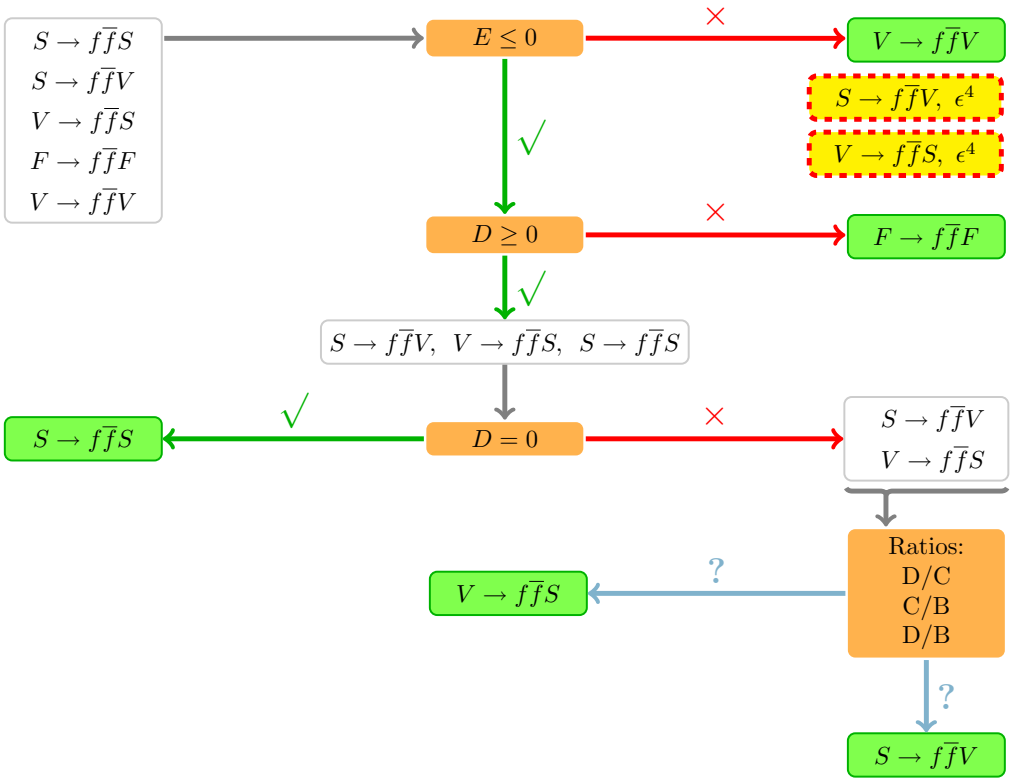

Figure 2: Flowchart for the strategy to discriminate different spin assignments for $m_f = 0$ using the signs of the coefficients given in section 3.1. Green (solid frame) boxes are for the case of taking only the leading order into account. Impact or dominance of higher order terms is given by the yellow (dashed frame) boxes, see text for details.

Let us first consider the case that X is in a non-trivial $SU(3)$ representation. Here only in the (S, S) there is a potentially dangerous contribution because the trilinear scalar coupling can in principle be of order m_I. However, from Eq. (A.3) we see that only the equality $B = C$ gets broken, the D-term will only get a tiny contribution, and thus the general strategy should still work. In case of the scalar exchange in the third topology of the (S, V) case the coupling is momentum dependent and is of order m_X and one is safe again. In the case X is a colour singlet all diagrams for the third topology in Table 1 contribute in principle. Here one has to distinguish two cases: (i) there are no new vector bosons or the new vector bosons do not belong to a new gauge group. In this case a detailed inspection of the diagrams shows that one arrives at the same conclusions as above, because all dimensionful couplings, which had not been considered before, have to be of the order m_X due to $SU_L(2)$ gauge invariance. (ii) There is a new gauge group at higher energies to which the intermediate vector bosons belong. In this case the SVV coupling as well as the masses of the vector boson will be of same order of magnitude and, thus, our

	(S,S)			(S,V)		(V,S)		(V,V)	
ϵ^4	s	c	1+2	s	$c/$ 1+2	s	$c/1+2$	s	$c/1+2$
B_4	+	+	0	+	+	+	+	+	+
C_4	±	+	0	±	±	±	−	±	±
D_4	+	0	0	±	−	±	±	−	−
E_4	0	0	0	+	+	+	+	+	+
F_4	0	0	0	0	0	0	0	+	+

Table 3: ϵ^4 coefficients for the case that ϵ^2, and thus also ϵ^3, are fine-tuned to vanish; $m_f = 0$.

assumption that the intermediate particle is much heavier than the decaying one does not hold in this case.

3.4 Special combinations of couplings

Up to now we have considered only the leading terms in case of decays of new bosons. However, it can happen that for special helicity assignments, the leading order ϵ^2 becomes zero. An example is the (S,S) case as can be seen in eqs. (A.3) and (A.4) where the leading order is proportional to $(g(r,s)n(l,s) + g(l,s)n(r,s))^2$ which is 0 in the case of e.g. $g(l,s) = n(r,s) = 0$. In such cases the $\not{p}/m_I^2$ part of the fermion propagator becomes important which contributes only at $\mathcal{O}(\epsilon^4)$. The question now is to which extent we would arrive at wrong conclusions using the strategy discussed so far. In table 3 we give the resulting signs of the coefficients which have to be compared with the $\mathcal{O}(\epsilon^2)$ coefficients of Table 2.
We start with the case where X is charged under $SU(3)$. One immediately sees that the cases (S,S) and (V,V) are not affected. The problematic ones are (S,V) and (V,S) which now get a positive E as is the case of (V,V) in the leading order. Unfortunately, ratios of the other coefficients do not help if one has no further information on couplings and/or masses of the intermediate particles. We have marked this possibility in Fig. 2 with the yellow boxes surrounded by red dashed lines. However, we want to stress that this requires fine-tuning between different couplings which although being unlikely, cannot be excluded on logical grounds.
In the case that X is a $SU(3)$ singlet the situation gets even a little bit more complicated, because now also in case of (S,S) the D coefficient is non-zero. However, it is still positive and, thus, it can for sure not be confused with the case of a new fermion. In the (V,V) case on the other hand we get in principle even more information as now also the F is non-zero which immediately tells us that there is a special combination of couplings.

3.5 Final states containing massive SM-fermions

Here we summarise the changes for massive SM-fermions, which in practice only is

	(S,S)		(S,V)		(V,S)		(V,V)	
ϵ^2	s	$c/1{+}2$	s	$c/\ 1{+}2$	s	$c/1{+}2$	s	$c/1{+}2$
A_2	0	0	$+$	$+$	$+$	$+$	$+$	$+$
B_2	$\pm$	$\pm$	$\pm$	$\pm$	$\pm$	$\pm$	$\pm$	$\pm$
C_2	$\pm$	$\pm$	$\pm$	$\pm$	$+$	$+$	$\pm$	$\pm$
D_2	0	0	$\pm$	$\pm$	$+$	$+$	$\pm$	$\pm$
E_2	0	0	0	0	0	0	$+$	$+$
ϵ^3								
A_3	0	0	$\pm$	$\pm$	$\pm$	$\pm$	$\pm$	$\pm$
B_3	$\pm$	$\pm$	$\pm$	$\pm$	$\pm$	$\pm$	$\pm$	$\pm$
C_3	$\pm$	$\pm$	$\pm$	$\pm$	$\pm$	$\pm$	$\pm$	$\pm$
D_3	0	0	$\pm$	$\pm$	$\pm$	$\pm$	$\pm$	$\pm$
E_3	0	0	0	0	0	0	$\pm$	$\pm$
ϵ^4								
Z_4	0	0	0	0	0	0	$-$	$-$
A_4	$+$	0	$+$	$+$	$+$	$+$	$+$	$+$
B_4	$\pm$	$+$	$\pm$	$\pm$	$\pm$	$\pm$	$\pm$	$\pm$
C_4	$\pm$	$+$	$\pm$	$\pm$	$\pm$	$\pm$	$\pm$	$\pm$
D_4	$\pm$	$-$	$\pm$	$\pm$	$\pm$	$\pm$	$\pm$	$\pm$
E_4	0	0	$\pm$	$\pm$	$\pm$	$\pm$	$\pm$	$\pm$
F_4	0	0	0	0	0	0	$\pm$	$\pm$

Table 4: Same as Table 2 but for massive SM-fermions.

	(S,S)			(S,V)		(V,S)		(V,V)	
ϵ^4	s	c	$1{+}2$	s	$c/1{+}2$	s	$c/1{+}2$	s	$c/1{+}2$
Z_4	0	0	0	0	0	0	0	$-$	$-$
A_4	$+$	0	0	$+$	$+$	$+$	$+$	$+$	$+$
B_4	$\pm$	$+$	$+$	$\pm$	$\pm$	$\pm$	$+$	$\pm$	$\pm$
C_4	$\pm$	$+$	$+$	$\pm$	$\pm$	$\pm$	$-$	$\pm$	$\pm$
D_4	$+$	0	0	$\pm$	$\pm$	$\pm$	$\pm$	$\pm$	$\pm$
E_4	0	0	0	$\pm$	$+$	$+$	$+$	$\pm$	$+$
F_4	0	0	0	0	0	0	0	$+$	$+$

Table 5: Same as Table 3 but $m_f \neq 0$.

important for top-quarks. The signs of the coefficients are given in Table 4. It turns out, that things hardly change but for the fact that one has to fit more coefficients.

Comparing tables 2 and 4 one sees that the same strategy can be used in principal. However, for distinguishing between the (S,V) and (V,S) cases the ranges for the ratios of the coefficients change. Moreover, only in the ratio D/C the unknown

couplings cancel and we find

$$\begin{aligned}(S,V): D/C &= \tfrac{(\tau_Y-1)^2-4\tau_f^2}{12\tau_f^2+22\tau_Y^2-4\tau_Y-2}\ \ [-\infty,-\tfrac{1}{3}]\cup[0,\infty]\\ (V,S): D/C &= \tfrac{(\tau_Y-1)^2-4\tau_f^2}{2\left(6\tau f^2-\tau_Y(\tau_Y+2)+11\right)}\ \ [0,\tfrac{1}{22}]\end{aligned} \tag{3.5}$$

where one has to use

$$1 \geq \tau_Y + 2\tau_f \tag{3.6}$$

due to total energy/momentum conservation. As in the case of massless SM-fermions, the overlap region of the two intervals is for the case $\tau_Y \to 1-2\tau_f$, e.g. the kinematical limit, where all particles are practically at rest in the centre of mass system of X. In general this ratio will be either negative or much larger than 1/2 in the (S,V) case. Note that we have $A = 0$ for the (S,S) case which, thus, serves as a confirmation of this case. Also in case of a new fermion we arrive at the same conclusions because

$$\text{sign}(A_4) = +\ \ , \ \ \text{sign}(B_4) = \pm\ \ , \ \ \text{sign}(C_4) = \pm\ \ , \ \ \text{sign}(D_4) = -\ \ , \ \ \text{sign}(E_4) = 0 \tag{3.7}$$

The only exception is where this decay is mediated solely by scalars in the third topology as in this case $A_4 = 0$.
For completeness, we also give the results in the case that the leading orders vanish in the case of decays of bosons in Table 5. It turns out that this case is the same as for the case of massless SM-fermions discussed above except that now in general also A will be non-zero.

3.6 Dependence on the mass of the intermediate particle(s)

We now address the question how small ϵ has to be so that our strategy works. For this we consider two examples: (I) $g(r) = g(l) = n(r) = n(l) = 1$ where the leading order dominates and (II) $g(r) = n(r) = 1$ but $g(l) = n(l) = 0$ so that the leading order vanishes in case of the bosonic decays and the subleading orders become dominant. Note, that in case of new fermions we did not manage to find a combination where the leading order vanishes. In all cases we have taken $m_X = 1\ TeV$, $m_Y = 100\ GeV$ and $m_f = 0$. We have checked that our results do not depend crucially on these values except for the cases where m_Y gets close to m_X which would imply soft SM fermions and experimental difficulties to observe the decay.
In figures 3 and 4 we show the relative deviation

$$R = \frac{d\,\Gamma_\epsilon - d\,\Gamma_H}{d\,\Gamma_H} \quad \text{with} \quad d\Gamma_i = \frac{1}{\Gamma_i}\frac{d\,\Gamma_i}{d\,\hat{s}}\ , \tag{3.8}$$

and H denotes the limit $m_I \to \infty$ and Γ_ϵ the differential width for a given ϵ. We find that for a decaying scalar and for a decaying fermion the deviation is always below

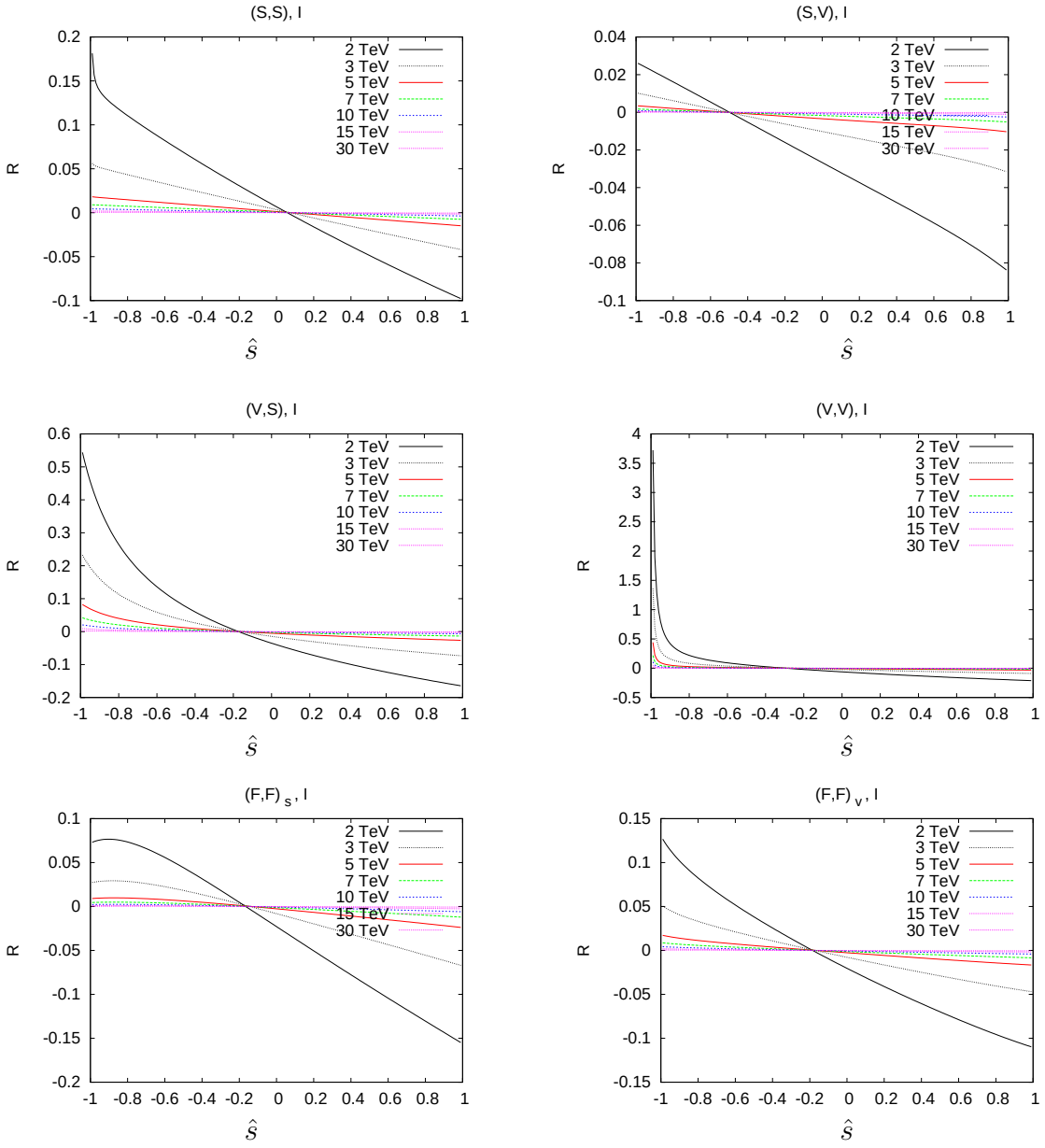

Figure 3: Ratio R for the processes $X \to f\bar{f}Y$ for scenario (i) taking $m_X = 1\ TeV$, $m_f = 0$, $m_Y = 0.1\ TeV$. We have calculated the decay width for the following masses of the intermediate particle: $m_I = 2, 3, 5, 7, 10, 15, 30\ TeV$.

20%. In case of a decaying vector particle the situation is more difficult and only for $\epsilon \leq 1/5$ we get $R \lesssim 0.2$ for all values of $\hat{s}$. The reason for these large deviations for $|\hat{s}|$ close to one is, that here the differential widths becomes zero and the rise/fall at the ends of the interval gets steeper the smaller ϵ is. This also implies, that in the corresponding intervals for $\hat{s}$ one will observe only a few events. The situation improves for a decay of a vector boson if the subleading terms become dominant as

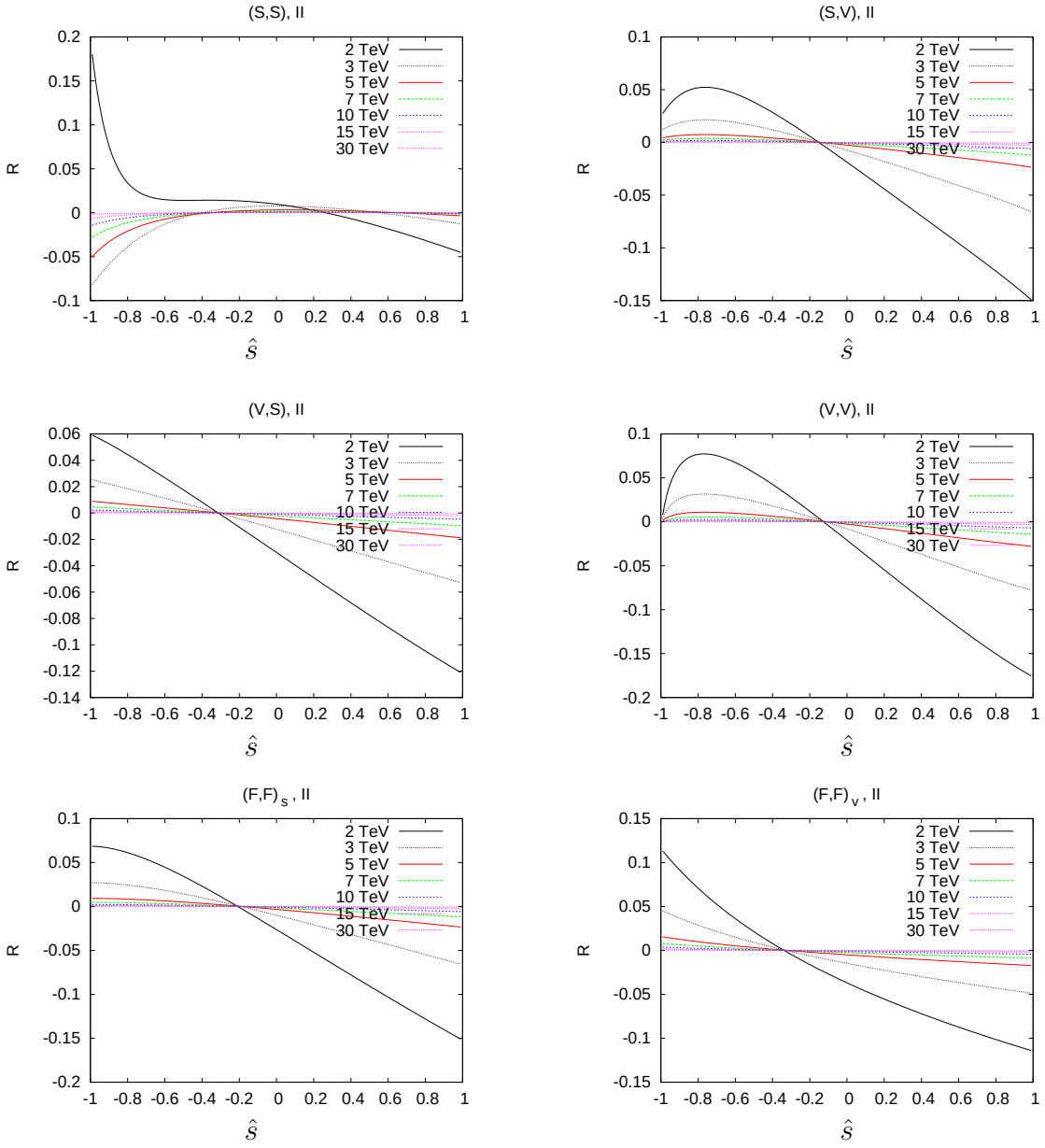

Figure 4: Relative deviation for differential decay width the processes $X \to f\bar{f}Y$ with couplings (II).

in Fig. 4.

In summary: our strategy should work well in all cases if ϵ is below $1/5$, in cases of scalar particles or spin $1/2$ fermion $\epsilon = 1/2$ is already a reasonable value. This is for example a natural value for gluino decays in supersymmetric models.

4. Testing our Strategy with Monte Carlo Simulations

We now test our strategy in Monte Carlo simulations at the parton level. For this one of us created data sets and the second one tried to find out the spin-assignments without any prior knowledge but m_Y and $(m_X - m_Y)$ and their uncertainties. We presume that the first one is given by an independent source with a precision of 10% and the second one with a precision of 3%. For definiteness we have taken $m_X = 1\,TeV$, $m_Y = 100\,GeV$ and $m_f = 0$. In the following we will denote by (B, C), (B, C, D), (B, C, D, E) and (B, C, D, E, F) the differential width in Eq. (3.1) where all but the given coefficients are zero.

4.1 Fitting procedure

In practice one will not have $\frac{d\Gamma}{d\hat{s}}(\hat{s})$ but one will have the number of events for a given interval $[\hat{s}_i, \hat{s}_i + \Delta\hat{s}]$. For this reason we actually fit 'distributions' of the form

$$\sum_{i=1}^{n} \int_{-1+(i-1)\Delta\hat{s}}^{-1+i\Delta\hat{s}} \frac{d\Gamma}{d\hat{s}} d\hat{s} \tag{4.1}$$

where $\Delta\hat{s} = 2/n$, n is the number of bins considered and $\frac{d\Gamma}{d\hat{s}}$ is given by Eq. (3.1). For the creation of the 'data' we have used our model file for generic particles and couplings [29] for the O'Mega/WHIZARD Monte Carlo generator [30, 31] which contains generic particles and couplings.
For fitting we use a linear least squares approach as described e.g. in [32] and the references given therein. We will exemplify this for the case of (B, C, D):

$$\begin{pmatrix} x_1 & x_1^2 & x_1^3 \\ x_2 & x_2^2 & x_2^3 \\ \vdots & & \\ x_n & x_n^2 & x_n^3 \end{pmatrix} \cdot \begin{pmatrix} B \\ C \\ D \end{pmatrix} = \hat{X} \cdot \begin{pmatrix} B \\ C \\ D \end{pmatrix} = \begin{pmatrix} \text{data}_1 \\ \text{data}_2 \\ \vdots \\ \text{data}_n \end{pmatrix} \tag{4.2}$$

where n is the number of bins. This equation can be solved by rewriting it as:

$$(\hat{X})^T \hat{X} \cdot \vec{c} = (\hat{X})^T \vec{d} \tag{4.3}$$

where $\vec{c} = (B, C, D)^T$ and $\vec{d}$ contains the 'measured' data of the differential width integrated over intervals of length $\Delta\hat{s}$. There are various methods to solve this equation, e.g. QR-decomposition. The fit is reliable if the matrix $(\hat{X})^T \hat{X}$ is well-conditioned, e.g. if its eigenvalues are of similar order of magnitude. After solving Eq. (4.3) we calculate the corresponding χ^2

$$\chi^2 = \frac{1}{n-j} \sum_i \frac{(\text{Expected}_i - \text{Observed}_i)^2}{\text{Expected}_i} \tag{4.4}$$

where n is the number of bins (= number of data points) and j the degrees of freedom (in this case the number of coefficients) of the fit function. We estimate the error for the coefficients by adding a Poisson noise to the data and determine the corresponding confidence interval after fitting.

4.2 A supersymmetric example

As a first test we study a focus point scenario which is inspired by SPS2 [33]: $m_0 = 3 \cdot 10^3$ GeV, $m_{1/2} = 3 \cdot 10^2$, $A_0 = 0$, $\tan\beta = 10$ and $\mathrm{sign}(\mu) > 0$. We simulate for the gluino decay 2k and 10k events and study also the effect of different binning sizes, namely 10 and 50 bins. Afterwards we fit the resulting distribution to all possible cases. Here we have assumed that the following information on the masses is given: $(m_X - m_Y) = 688 \pm 23\ GeV$, $m_Y = 121 \pm 12\ GeV$ with a Gaussian distribution. The results are summarised in Table 6. As one does not know neither the absolute values of the couplings nor the intermediate masses, one has the freedom to normalise B to 1 and, thus, only the other coefficients and their uncertainties are given. The χ^2 favours for both 10 and 50 bins slightly the (B, C, D) polynomial. However, if higher powers in $\hat{s}$ are included, one still obtains a good fit and the χ^2 will not be sufficient to discriminate between the different possibilities. This is a quite generic feature because usually there is a hierarchy between the non-zero coefficients: $|B|, |C| \gg |E|, |F|$. The (B, C) case can be ruled out since $B \neq C$ within the range of the error bars. The smallness of the parameters and the large errors on the E and F coefficients of the (B, C, D, E) and (B, C, D, E, F) models suggest that those values are zero. The remaining model is (B, C, D) with negative D which suggests (F, F). We find it encouraging that one gets already for 2000 events first information including that the (S, S) case can be excluded.

4.3 Large sample tests

In the second step we have tested our strategy for a large set of random couplings fixing however the kinematics to $m_X = 1\ TeV$, $m_Y = 100\ GeV$ and all $m_I = 15\ TeV$. The latter number is not crucial as long as it is above 5 TeV (2 TeV) in case of decaying vector bosons (decaying scalars and fermions). We have generated 100 different sets with random couplings for each of the decays (S, S), (S, V), (V, S), (V, V) and (F, F) and we have generated for each set of couplings 10^4, 10^5 and 10^6 events. In an ideal world one could use the strategy depicted in Fig. 2 without any problems. In reality there will be some smearing of the data from the measurement itself as well as from the background subtraction. To be sure that we do not miss anything we have slightly advanced our strategy and apply it to the following model list

$$\{(S, S), (S, V), (V, S), (F, F), (V, V), (V, V)_4\} \tag{4.5}$$

Coef.	χ^2	$(\mathrm{F,F})_{10}$	χ^2	$(\mathrm{F,F})_{50}$	χ^2	$(\mathrm{F,F})_{10,2k}$
C	5.9	0.210 ± 0.061	1.50	0.208 ± 0.071	1.58	0.208 ± 0.126
C	0.55	0.089 ± 0.077	0.62	0.089 ± 0.076	1.55	0.089 ± 0.155
D		-0.232 ± 0.106		-0.227 ± 0.110		-0.227 ± 0.252
C	0.63	0.079 ± 0.141	0.63	0.067 ± 0.128	1.75	0.067 ± 0.300
D		-0.218 ± 0.150		-0.197 ± 0.139		-0.197 ± 0.322
E		0.028 ± 0.227		0.060 ± 0.228		0.060 ± 0.536
C	0.75	0.080 ± 0.149	0.64	0.077 ± 0.160	1.14	0.077 ± 0.401
D		-0.215 ± 0.456		-0.169 ± 0.340		-0.169 ± 1.108
E		0.025 ± 0.260		0.035 ± 0.311		0.035 ± 0.738
F		-0.006 ± 0.516		-0.046 ± 0.443		-0.046 ± 1.315

Table 6: Testing of the SUSY focus point taking 10 bins in case of 2000 events and 10 and 50 bins for 10000 events. Input for the fit is: $(m_X - m_Y) = 688 \pm 23\ GeV$, $m_Y = 121 \pm 12\ GeV$ with gaussian distribution, $m_I = 3026\ GeV$. The coefficients are normalised such that $B = 1$ and the uncertainties are at 3σ. The analytic values for the coefficients are $B = 1$, $C = 0.123$, $D = -0.188$.

and the corresponding differential widths. $(V,V)_4$ denotes the case, where only the 4th order in ϵ of (V,V) remains. We have tested for the following criterions:

1. $B \neq C \rightarrow$ remove (S,S)
2. $D > 0 \rightarrow$ remove (F,F); $D < 0 \rightarrow$ remove $(S,V),(V,S)$
3. C/B in (S,V) interval $\rightarrow$ if not remove (S,V)
4. C/B in (V,S) interval $\rightarrow$ if not remove (V,S)
5. D/B in (S,V) interval $\rightarrow$ if not remove (S,V)
6. D/B in (V,S) interval $\rightarrow$ if not remove (V,S)
7. D/C in (S,V) interval $\rightarrow$ if not remove (S,V)
8. D/C in (V,S) interval $\rightarrow$ if not remove (V,S)
9. if $E < 0$ in $(V,V)/(V,V)_4$, $\rightarrow$ remove $(V,V)/(V,V)_4$
10. if $F < 0$ in $(V,V)_4$, $\rightarrow$ remove $(V,V)_4$
11. Optional: Remove all models with $\chi^2 > 3$
12. Optional: Remove $(V,V)/(V,V)_4$ if $E, F < 0.001$ respectively

Every time one criterion could be applied or not fulfilled within the range of the error bars, the corresponding model was cancelled from the list in Eq. (4.5).

In table 7 we have summarised our results for these different Monte Carlo data sets where we give the number of the remaining models after going through the different criteria. The first row e.g. means, that we started with 100 different data sets for the (S,S) decay, applied our tests and after that, 100 (S,S) models remained, 0 of (S,V), 20 of (V,S), 100 of (F,F) and so on. There were no data sets where only a wrong model remained.

	(S,S)	(S,V)	(V,S)	(F,F)	(V,V)	(V,V_4)
10^4 events:						
(S,S):	**100**	0	20	100	100	100
(S,V):	0	**99**	0	1	100	99
(V,S):	0	0	**99**	99	100	98
(F,F):	0	5	0	**100**	99	99
(V,V):	0	66	0	78	**100**	100
10^5 events:						
(S,S):	**100**	0	0	100	100	100
(S,V):	0	**99**	0	0	100	100
(V,S):	0	0	**100**	100	100	100
(F,F):	0	0	0	**100**	100	100
(V,V):	0	66	0	78	**100**	100
10^6 events:						
(S,S):	**100**	0	0	100	100	100
(S,V):	0	**98**	0	0	99	100
(V,S):	0	0	**100**	100	100	100
(F,F):	0	0	0	**100**	100	100
(V,V):	0	10	0	61	**100**	100

Table 7: Number for the remaining models for 100 input models each where the various criterions are applied using 3σ uncertainties on the coefficients. The masses are chosen as $m_Y = 100 \pm 10\ GeV$ and the mass difference $(m_X - m_Y) = 900 \pm 30\ GeV$. The bold numbers are the correct model fits.

The obtained results can be understood as follows: (i) It is easier to fit a polynomial which has low powers of $\hat{s}$ by a higher order polynomial if there is smearing than vice versa. (ii) The number of criterions depend on the decay mode, e.g. it is easier to exclude (S,V) where 3 criterions are at hand than (V,V) where only one exists. (iii) The modulus of the coefficients E and F is usually up to two orders of magnitude smaller than the modulus of the other coefficients but the absolute uncertainty is roughly the same for all coefficients. In particular the third item implies that it will

	(S,S)	(S,V)	(V,S)	(F,F)	(V,V)	(V,V_4)
10^4 events:						
(S,S):	**99/100**	0/0	19/20	99/100	99/85	97/90
(S,V):	0/0	**96/96**	0/0	0/1	93/95	90/89
(V,S):	0/0	0/0	**97/97**	97/99	99/88	96/81
(F,F):	0/0	5/5	/00	**98/100**	98/89	97/87
(V,V):	0/0	46/66	0/0	31/78	**95/95**	92/90
10^5 events:						
(S,S):	**100/99**	0/0	0/0	100/100	97/63	98/63
(S,V):	0/0	**99/95**	0/0	0/0	97/81	94/72
(V,S):	0/0	0/0	**100/100**	100/100	100/66	99/64
(F,F):	0/0	0/0	0/0	**99/100**	98/66	98/61
(V,V):	0/0	46/66	0/0	31/78	**95/95**	92/90
10^6 events:						
(S,S):	**100/100**	0/0	0/0	100/99	100/14	96/23
(S,V):	0/0	95/98	0/0	0/0	93/54	90/33
(V,S):	0/0	0/0	**99/100**	99/100	98/17	98/28
(F,F):	0/0	0/0	0/0	**100/100**	98/22	97/25
(V,V):	0/0	0/10	0/0	0/61	**93/100**	97/64

Table 8: Same as Table 7 but taking into account either the optional criterion 11 (exclude $\chi^2 > 3$) or criterion 12 (small E,F) corresponding to the first and second number given at the various entries.

be rather difficult to exclude a positive E and F in practice if only one decay channel is considered.

Additionally we have also looked at the optional criteria item 11 and 12 separately and give the resulting numbers in Table 8. The first number of 99/100 (as e.g. in the (S,S) case) denotes the number remaining after applying the χ^2 criterion, the second number the same with the small E,F criterion. The results are (i) the $\chi^2 > 3$ criterion is most useful if the underlying decay is $(V,V)/(V,V)_4$, since the polynomials with a lower order have a large χ^2. This is e.g. reflected in the (V,V) decay with 10k events, and the fitted (S,V) and (F,F) polynomials. Here the number of remaining processes are reduced by applying the χ^2 test from 66 ((S,V), Table 7) to 46 (Table 8) and for (F,F) from 78 to 31. (ii) The criterion for small E,F works very good for high statistics since the fit gives values close to 0. This is reflected in the last row of Table 8, where the underlying process is (F,F). After applying of the common criterions, 100 of (V,V) and 100 of $(V,V)_4$ models remain (see Table 7). But after applying additionally the criterion item 12 this number is reduced to 22 (V,V) and 25 $(V,V)_4$. However, the same argument does not remove any of the (V,V) models, if (V,V) is the underlying process. For a smaller number of events, there are only

a view coefficients E, F smaller then 0.001 so only a smaller number of models are removed as e.g. in Table 8 for 10k events, 88/81 remaining $(V,V)/(V,V)_4$ models for the underlying (V,S) process.
Since our decision making strategy depends upon the correct error estimation of the coefficients, we have independently checked that the Markov-Chain-Monte-Carlo (MCMC) method for the data fitting which yields roughly the same errors on the coefficients.

5. Conclusions

In this paper we have investigated three-body decays of the form $X \to f\bar{f}Y$ where X and Y are new particles and f are SM-fermions with the aim to determine the spins of the new particles. Here we assumed that Y is a DM candidate and escapes detection in a typical LHC detector.
We have studied in detail the differential width as a function of the invariant mass of the SM-fermions for the case of heavy intermediate particles with mass m_I and expanded the width in powers of the ratio $\epsilon = m_X/m_I$. It turns out that general properties such as signs or various ratios of the resulting coefficients depend on the spin assignments of X and Y. From this we have developed a strategy for the spin identification discussing various cases and testing it on large samples of arbitrary coupling assignments. Here it turns out that one is able to exclude several spin assignments but one does not get necessarily find a unique solution once one has to deal with noisy data.
Although we did not find a unique solution we are convinced that the proposed method will be useful in practice for the following reasons: (i) We have only investigated one particular decay channel. However, in general several channels will be open which can be combined. (ii) In the same spirit: we have only investigated one decaying particle. In practice, e.g. if supersymmetry or extra dimensions are realized in nature, several distinct new particles will be produced which eventually have to decay into the lightest of the new ones if a parity like R-parity or KK-parity is realized. Therefore, one will have several different possibilities to determine the spin of the invisible particle Y. (iii) Our information can be combined with other observables, e.g. with cross section information. However, here one most likely will have to assume a certain representation to which a particular new particle belongs, e.g. if it is an $SU(3)$ triplet or octet.

Acknowledgements

We thank R. Ströhmer for useful discussions. This work has been supported by the German Ministry of Education and Research (BMBF) under contract no. 05H09WWE. L.E. acknowledges support from the Elitenetzwerk Bayern.

A. Analytic Results for the Coefficients

The coefficients of the differential decay widths are given below. We restrict ourselves to the case of massless SM-fermions, implying that $Z = A = 0$ and, thus, the differential widths read as

$$\frac{d\Gamma}{d\hat{s}} = \frac{PS}{(2\pi)^3\ 256\ m_X}\left(B + C\hat{s} + D\hat{s}^2 + E\hat{s}^3 + F\hat{s}^4\right) \tag{A.1}$$

A.1 Decays of new bosons

The coefficients are shown with all possible diagrams and vertices in Table 1. For the definition of ϵ and the various τ_i see Eq. (2.2). We give the various orders separately, e.g.

$$B = \sum_{j=2}^{4} B_j \epsilon^j \tag{A.2}$$

For brevity, we only explicitely write out the higher orders for (S, S).

$\underline{S \to f\overline{f}S}$**:**

$$\begin{aligned}
B_2 &= 128\epsilon^2(\tau_Y - 1)^2(g(r,s)n(l,s) + g(l,s)n(r,s))^2 \\
C_2 &= 128\epsilon^2(\tau_Y - 1)^2(g(r,s)n(l,s) + g(l,s)n(r,s))^2 \\
D_2 &= 0
\end{aligned} \tag{A.3}$$

$$\begin{aligned}
B_3 &= 64\epsilon^3\tau_C(\tau_Y - 1)^2 c(s)(g(r,s)n(l,s) + g(l,s)n(r,s))(s(l) + s(r)) \\
C_3 &= 64\epsilon^3\tau_C(\tau_Y - 1)^2 c(s)(g(r,s)n(l,s) + g(l,s)n(r,s))(s(l) + s(r)) \\
D_3 &= 0
\end{aligned} \tag{A.4}$$

$$\begin{aligned}
B_4 = \frac{16}{3}\epsilon^4(\tau_Y - 1)^2 \big(&12g(r,s)^2 n(l,s)^2(\tau_Y + 1)^2 + 12g(l,s)^2 n(r,s)^2(\tau_Y + 1)^2 \\
&+24g(l,s)g(r,s)n(l,s)n(r,s)(\tau_Y + 1)^2 + 3\tau_C^2 c(s)^2 s(l)^2 + 3\tau_C^2 c(s)^2 s(r)^2 \\
&+\tau_Y^2 c(v)^2 v(l)^2 + 6\tau_Y c(v)^2 v(l)^2 + c(v)^2 v(l)^2 + \tau_Y^2 c(v)^2 v(r)^2 \\
&+6\tau_Y c(v)^2 v(r)^2 + c(v)^2 v(r)^2\big) \\
C_4 = -\frac{16}{3}\epsilon^4(\tau_Y - 1)^2 \big(&-48\tau_Y g(r,s)^2 n(l,s)^2 - 96\tau_Y g(l,s)g(r,s)n(r,s)n(l,s) \\
&-48\tau_Y g(l,s)^2 n(r,s)^2 - 3\tau_C^2 c(s)^2 s(l)^2 - 3\tau_C^2 c(s)^2 s(r)^2 + 2\tau_Y^2 c(v)^2 v(l)^2 \\
&+4\tau_Y c(v)^2 v(l)^2 + 2c(v)^2 v(l)^2 + 2\tau_Y^2 c(v)^2 v(r)^2 \\
&+4\tau_Y c(v)^2 v(r)^2 + 2c(v)^2 v(r)^2\big) \\
D_4 = -\frac{16}{3}\epsilon^4(\tau_Y - 1)^4 \big(&-\left(v(l)^2 + v(r)^2\right) c(v)^2 + 12g(r,s)^2 n(l,s)^2 \\
&+12g(l,s)^2 n(r,s)^2 + 24g(l,s)g(r,s)n(l,s)n(r,s)\big)
\end{aligned} \tag{A.5}$$

Moreover, we get $E_j = 0$ in all orders considered.

$\underline{S \to f\overline{f}V\textbf{:}}$

$$
\begin{aligned}
B_2 &= \frac{64}{3\tau_Y^2}\left(g(r,s)^2 n(l,v)^2 + g(l,s)^2 n(r,v)^2\right)\epsilon^2(\tau_Y-1)^2\left(25\tau_Y^2+6\tau_Y+1\right)\\
C_2 &= \frac{128}{3\tau_Y^2}\left(g(r,s)^2 n(l,v)^2 + g(l,s)^2 n(r,v)^2\right)\epsilon^2(\tau_Y-1)^2\left(11\tau_Y^2-2\tau_Y-1\right)\\
D_2 &= \frac{64}{3\tau_Y^2}\left(g(r,s)^2 n(l,v)^2 + g(l,s)^2 n(r,v)^2\right)\epsilon^2(\tau_Y-1)^4
\end{aligned}
\tag{A.6}
$$

$\underline{V \to f\overline{f}S\textbf{:}}$

$$
\begin{aligned}
B_2 &= \frac{64}{3}\left(g(r,v)^2 n(l,s)^2 + g(l,v)^2 n(r,s)^2\right)\epsilon^2(\tau_Y-1)^2\left(\tau_Y^2+6\tau_Y+25\right)\\
C_2 &= -\frac{128}{3}\left(g(r,v)^2 n(l,s)^2 + g(l,v)^2 n(r,s)^2\right)\epsilon^2(\tau_Y-1)^2\left(\tau_Y^2+2\tau_Y-11\right)\\
D_2 &= \frac{64}{3}\left(g(r,v)^2 n(l,s)^2 + g(l,v)^2 n(r,s)^2\right)\epsilon^2(\tau_Y-1)^4
\end{aligned}
\tag{A.7}
$$

$\underline{V \to f\overline{f}V\textbf{:}}$

$$
\begin{aligned}
B_2 &= \frac{32}{3\tau_Y^2}\epsilon^2(\tau_Y-1)^2\Big(g(r,v)^2\left(3\tau_Y^4+16\tau_Y^3+54\tau_Y^2+16\tau_Y+3\right)n(l,v)^2\\
&\quad -g(l,v)g(r,v)n(r,v)\left(3\tau_Y^4+20\tau_Y^3-6\tau_Y^2+20\tau_Y+3\right)n(l,v)\\
&\quad +g(l,v)^2 n(r,v)^2\left(3\tau_Y^4+16\tau_Y^3+54\tau_Y^2+16\tau_Y+3\right)\Big)\\
C_2 &= -\frac{32}{3\tau_Y^2}\epsilon^2(\tau_Y-1)^2\Big(g(r,v)^2\left(5\tau_Y^4+4\tau_Y^3-46\tau_Y^2+4\tau_Y+5\right)n(l,v)^2\\
&\quad -g(l,v)g(r,v)n(r,v)\left(7\tau_Y^4+20\tau_Y^3+34\tau_Y^2+20\tau_Y+7\right)n(l,v)\\
&\quad +g(l,v)^2 n(r,v)^2\left(5\tau_Y^4+4\tau_Y^3-46\tau_Y^2+4\tau_Y+5\right)\Big)\\
D_2 &= \frac{32}{3\tau_Y^2}\epsilon^2(\tau_Y-1)^4\Big(g(r,v)^2\left(\tau_Y^2-6\tau_Y+1\right)n(l,v)^2\\
&\quad -g(l,v)g(r,v)n(r,v)\left(5\tau_Y^2+6\tau_Y+5\right)n(l,v)\\
&\quad +g(l,v)^2 n(r,v)^2\left(\tau_Y^2-6\tau_Y+1\right)\Big)\\
E_2 &= \frac{32}{3\tau_Y^2}\left(g(r,v)^2 n(l,v)^2 + g(l,v)g(r,v)n(r,v)n(l,v) + g(l,v)^2 n(r,v)^2\right)\epsilon^2(\tau_Y-1)^6
\end{aligned}
\tag{A.8}
$$

A.2 Decays of new fermions

As noted before, in this case only the 4th order in ϵ contributes. We split the various coefficients according to the different topologies considered, e.g. the scalar contributions to B_4 are

$$B_4 = B_s + B'_s + B_{s,m} \tag{A.9}$$

where

B_s : top. 1+2 with intermediate scalars

B'_s : top. 3 with intermediate scalars

$B_{s,m}$: interference term of top. (1+2)+3 with intermediate scalars

For intermediate vector bosons the index v is used. For the interference terms between scalars and vector bosons the index (sv) is used in case of topologies 1+2, $(sv1)$ for the scalars of topology 1+2 and vector bosons of topology 3, $(s1v)$ for the scalars of topology 3 and vector bosons of topology 1+2. Moreover we find that the interference vanishes if both, scalars and vector bosons stem from the third topology because we have $m_f = 0$ for the SM-fermions.

Intermediate scalars:

$$\begin{aligned}
B_s &= \frac{64}{3}(\tau_Y-1)^2\Big(2\Big((\tau_Y(\tau_Y+6)+1)n(l,s)^2+(\tau_Y(\tau_Y+3)+1)n(r,s)^2\Big)g(l,s)^2\\
&\quad -(\tau_Y(\tau_Y+6)+1)g(r,s)n(l,s)n(r,s)g(l,s)+2g(r,s)^2\Big((\tau_Y(\tau_Y+3)+1)n(l,s)^2\\
&\quad +(\tau_Y(\tau_Y+6)+1)n(r,s)^2\Big)\Big)\\
C_s &= -\frac{64}{3}(\tau_Y-1)^2\Big(-2g(l,s)g(r,s)n(l,s)n(r,s)(\tau_Y+1)^2\\
&\quad +g(r,s)^2\Big(((\tau_Y-4)\tau_Y+1)n(l,s)^2+((\tau_Y-10)\tau_Y+1)n(r,s)^2\Big)\\
&\quad +g(l,s)^2\Big(((\tau_Y-10)\tau_Y+1)n(l,s)^2+((\tau_Y-4)\tau_Y+1)n(r,s)^2\Big)\Big)\\
D_s &= -\frac{64}{3}(\tau_Y-1)^4\Big(\Big(n(l,s)^2+n(r,s)^2\Big)g(l,s)^2\\
&\quad +g(r,s)n(l,s)n(r,s)g(l,s)+g(r,s)^2\Big(n(l,s)^2+n(r,s)^2\Big)\Big)
\end{aligned} \tag{A.10}$$

$$\begin{aligned}
B'_s &= 32(\tau_Y-1)^2\Big((\tau_Y+1)^2d(l,s)^2\\
&\quad +8\tau_Y d(r,s)d(l,s)+(\tau_Y+1)^2d(r,s)^2\Big)\Big(s(l)^2+s(r)^2\Big)\\
C'_s &= 128(\tau_Y-1)^2\tau_Y(d(l,s)+d(r,s))^2\Big(s(l)^2+s(r)^2\Big)\\
D'_s &= -32(\tau_Y-1)^4\Big(d(l,s)^2+d(r,s)^2\Big)\Big(s(l)^2+s(r)^2\Big)
\end{aligned} \tag{A.11}$$

$$\begin{aligned}
B_{s,m} &= -32(\tau_Y-1)^2(g(r,s)n(l,s)+g(l,s)n(r,s))\Big(d(r,s)\Big(s(l)(\tau_Y+1)^2+4\tau_Y s(r)\Big)\\
&\quad +d(l,s)\Big(s(r)(\tau_Y+1)^2+4\tau_Y s(l)\Big)\Big)\\
C_{s,m} &= -128(\tau_Y-1)^2\tau_Y(g(r,s)n(l,s)+g(l,s)n(r,s))(d(l,s)+d(r,s))(s(l)+s(r))\\
D_{s,m} &= 32(\tau_Y-1)^4(g(r,s)n(l,s)+g(l,s)n(r,s))(d(r,s)s(l)+d(l,s)s(r))
\end{aligned} \tag{A.12}$$

Intermediate vector bosons:

$$\begin{aligned}
B_v &= \frac{256}{3}(\tau_Y-1)^2\Big(6g(l,v)g(r,v)n(l,v)n(r,v)(\tau_Y+1)^2\\
&\quad +g(l,v)^2\Big(2(\tau_Y(\tau_Y+6)+1)n(l,v)^2+3(\tau_Y+1)^2n(r,v)^2\Big)\\
&\quad +g(r,v)^2\Big(3(\tau_Y+1)^2n(l,v)^2+2(\tau_Y(\tau_Y+6)+1)n(r,v)^2\Big)\Big)
\end{aligned}$$

$$
\begin{aligned}
C_v &= \frac{256}{3}(\tau_Y-1)^2\left(\left(12\tau_Y n(r,v)^2-((\tau_Y-10)\tau_Y+1)n(l,v)^2\right)g(l,v)^2\right.\\
&\quad\left.+24\tau_Y g(r,v)n(l,v)n(r,v)g(l,v)+g(r,v)^2\left(12\tau_Y n(l,v)^2-((\tau_Y-10)\tau_Y+1)n(r,v)^2\right)\right)\\
D_v &= -\frac{256}{3}(\tau_Y-1)^4\left(\left(n(l,v)^2+3n(r,v)^2\right)g(l,v)^2\right.\\
&\quad\left.+6g(r,v)n(l,v)n(r,v)g(l,v)+g(r,v)^2\left(3n(l,v)^2+n(r,v)^2\right)\right)
\end{aligned}
\tag{A.13}
$$

$$
\begin{aligned}
B'_v &= \frac{256}{3}(\tau_Y-1)^2\left((\tau_Y(\tau_Y+3)+1)d(l,v)^2-6\tau_Y d(r,v)d(l,v)\right.\\
&\quad\left.+(\tau_Y(\tau_Y+3)+1)d(r,v)^2\right)\left(v(l)^2+v(r)^2\right)\\
C'_v &= -\frac{128}{3}(\tau_Y-1)^2\left(((\tau_Y-4)\tau_Y+1)d(l,v)^2\right.\\
&\quad\left.+12\tau_Y d(r,v)d(l,v)+((\tau_Y-4)\tau_Y+1)d(r,v)^2\right)\left(v(l)^2+v(r)^2\right)\\
D'_v &= -\frac{128}{3}(\tau_Y-1)^4\left(d(l,v)^2+d(r,v)^2\right)\left(v(l)^2+v(r)^2\right)
\end{aligned}
\tag{A.14}
$$

$$
\begin{aligned}
B_{v,m} &= \frac{512}{3}(\tau_Y-1)^2(\tau_Y(\tau_Y+6)+1)(d(l,v)-d(r,v))\\
&\quad(g(l,v)n(l,v)v(l)-g(r,v)n(r,v)v(r))\\
C_{v,m} &= -\frac{256}{3}(\tau_Y-1)^2((\tau_Y-10)\tau_Y+1)(d(l,v)-d(r,v))\\
&\quad(g(l,v)n(l,v)v(l)-g(r,v)n(r,v)v(r))\\
D_{v,m} &= -\frac{256}{3}(\tau_Y-1)^4(d(l,v)-d(r,v))(g(l,v)n(l,v)v(l)-g(r,v)n(r,v)v(r))
\end{aligned}
\tag{A.15}
$$

Interference terms between scalars and vector bosons:

$$
\begin{aligned}
B_{sv} &= -\frac{512}{3}(\tau_Y-1)^2(n(l,v)(3\tau_Y g(l,s)g(r,v)n(r,s)+g(r,s)(3\tau_Y g(r,v)n(l,s)\\
&\quad+(\tau_Y(\tau_Y+6)+1)g(l,v)n(r,s)))+((\tau_Y(\tau_Y+6)+1)g(l,s)g(r,v)n(l,s)\\
&\quad+3\tau_Y g(l,v)(g(r,s)n(l,s)+g(l,s)n(r,s)))n(r,v))\\
C_{sv} &= \frac{256}{3}(\tau_Y-1)^2(n(l,v)(g(r,s)(((\tau_Y-10)\tau_Y+1)g(l,v)n(r,s)\\
&\quad-6\tau_Y g(r,v)n(l,s))-6\tau_Y g(l,s)g(r,v)n(r,s))+(((\tau_Y-10)\tau_Y+1)g(l,s)g(r,v)n(l,s)\\
&\quad-6\tau_Y g(l,v)(g(r,s)n(l,s)+g(l,s)n(r,s)))n(r,v))\\
D_{sv} &= \frac{256}{3}(\tau_Y-1)^4(g(l,v)g(r,s)n(l,v)n(r,s)+g(l,s)g(r,v)n(l,s)n(r,v))
\end{aligned}
\tag{A.16}
$$

$$
\begin{aligned}
B_{sv1} &= -\frac{256}{3}(\tau_Y-1)^2(\tau_Y(\tau_Y+6)+1)(d(l,v)-d(r,v))\\
&\quad(g(r,s)n(r,s)v(l)-g(l,s)n(l,s)v(r))
\end{aligned}
$$

$$
\begin{aligned}
C_{sv1} &= \frac{128}{3}(\tau_Y-1)^2((\tau_Y-10)\tau_Y+1)(d(l,v)-d(r,v)) \\
&\quad (g(r,s)n(r,s)v(l)-g(l,s)n(l,s)v(r)) \\
D_{sv1} &= \frac{128}{3}(\tau_Y-1)^4(d(l,v)-d(r,v))(g(r,s)n(r,s)v(l)-g(l,s)n(l,s)v(r))
\end{aligned}
\tag{A.17}
$$

$$
\begin{aligned}
B_{s1v} &= 128(\tau_Y-1)^2(g(r,v)n(l,v)+g(l,v)n(r,v))\left(d(l,s)\left(s(l)(\tau_Y+1)^2+4\tau_Y s(r)\right)\right. \\
&\quad \left.+d(r,s)\left(s(r)(\tau_Y+1)^2+4\tau_Y s(l)\right)\right) \\
C_{s1v} &= 512(\tau_Y-1)^2\tau_Y(g(r,v)n(l,v)+g(l,v)n(r,v)) \\
&\quad (d(l,s)+d(r,s))(s(l)+s(r)) \\
D_{s1v} &= -128(\tau_Y-1)^4(g(r,v)n(l,v)+g(l,v)n(r,v))(d(l,s)s(l)+d(r,s)s(r))
\end{aligned}
\tag{A.18}
$$

References

[1] S. Y. Choi, D. J. Miller, 2, M. M. Muhlleitner, and P. M. Zerwas. Identifying the Higgs spin and parity in decays to Z pairs. *Phys. Lett.*, B553:61–71, 2003.

[2] A. Alves, O. J. P. Eboli, M. C. Gonzalez-Garcia, and J. K. Mizukoshi. Deciphering the spin of new resonances in Higgsless models. *Phys. Rev.*, D79:035009, 2009.

[3] P. Osland, A. A. Pankov, N. Paver, and A. V. Tsytrinov. Spin identification of the Randall-Sundrum resonance in lepton-pair production at the LHC. *Phys. Rev.*, D78:035008, 2008.

[4] P. Osland, A. A. Pankov, A. V. Tsytrinov, and N. Paver. Spin and model identification of Z' bosons at the LHC. *Phys. Rev.*, D79:115021, 2009.

[5] A. J. Barr. Measuring slepton spin at the LHC. *JHEP*, 02:042, 2006.

[6] J. M. Smillie and B. R. Webber. Distinguishing Spins in Supersymmetric and Universal Extra Dimension Models at the Large Hadron Collider. *JHEP*, 10:069, 2005.

[7] C. Athanasiou, C. G. Lester, J. M. Smillie, and B. R. Webber. Distinguishing spins in decay chains at the Large Hadron Collider. *JHEP*, 08:055, 2006.

[8] C. Athanasiou, C. G. Lester, J. M. Smillie, and B. R. Webber. Addendum to 'Distinguishing spins in decay chains at the Large Hadron Collider'. *hep-ph*/0606212. 2006.

[9] J. M. Smillie. Spin Correlations in Decay Chains Involving W Bosons. *Eur. Phys. J.*, C51:933–943, 2007.

[10] L.-T. Wang and I. Yavin. Spin Measurements in Cascade Decays at the LHC. *JHEP*, 04:032, 2007.

[11] P. Meade and M. Reece. Top partners at the LHC: Spin and mass measurement. *Phys. Rev.*, D74:015010, 2006.

[12] C. Kilic, L.-T. Wang, and I. Yavin. On the Existence of Angular Correlations in Decays with Heavy Matter Partners. *JHEP*, 05:052, 2007.

[13] A. Alves and O. Eboli. Unravelling the sbottom spin at the CERN LHC. *Phys. Rev.*, D75:115013, 2007.

[14] A. Rajaraman and B. T. Smith. Determining Spins of Metastable Sleptons at the Large Hadron Collider. *Phys. Rev.*, D76:115004, 2007.

[15] W. S. Cho, K. Choi, Y. Gy. Kim, and C. B. Park. M_{T2}-assisted on-shell reconstruction of missing momenta and its application to spin measurement at the LHC. *Phys. Rev.*, D79:031701, 2009.

[16] L.-T. Wang and I. Yavin. A Review of Spin Determination at the LHC. *Int. J. Mod. Phys.*, A23:4647–4668, 2008.

[17] M. Burns, K. Kong, K. T. Matchev, and M. Park. A General Method for Model-Independent Measurements of Particle Spins, Couplings and Mixing Angles in Cascade Decays with Missing Energy at Hadron Colliders. *JHEP*, 10:081, 2008.

[18] G. L. Kane, A. A. Petrov, J. Shao, and L.-T. Wang. Initial determination of the spins of the gluino and squarks at LHC. *J. Phys.*, G37:045004, 2010.

[19] C. Csaki, J. Heinonen, and M. Perelstein. Testing Gluino Spin with Three-Body Decays. *JHEP*, 10:107, 2007.

[20] M. R. Buckley, H. Murayama, W. Klemm and V. Rentala, Discriminating spin through quantum interference. *Phys. Rev.*, D78:014028, 2008.

[21] M. R. Buckley, B. Heinemann, W. Klemm and H. Murayama, Quantum Interference Effects Among Helicities at LEP-II and Tevatron. *Phys. Rev.*, D77:113017, 2008.

[22] M. R. Buckley, S. Y. Choi, K. Mawatari and H. Murayama, Determining Spin through Quantum Azimuthal-Angle Correlations. *Phys. Lett.*, B672:275–279, 2009.

[23] F. Boudjema and R. K. Singh, A model independent spin analysis of fundamental particles using azimuthal asymmetries, *JHEP*, 28:907, 2009

[24] G. F. Giudice and A. Romanino. Split supersymmetry. *Nucl. Phys.*, B699:65–89, 2004.

[25] S. C. Park and J. Shu. Split-UED and Dark Matter. *Phys. Rev.*, D79:091702, 2009.

[26] A. Knochel and T. Ohl. Supersymmetric Extensions and Dark Matter in Models of Warped Higgsless EWSB. *Phys. Rev.*, D78:045016, 2008.

[27] A. Alves, O. Eboli, and T. Plehn. It's a gluino. *Phys. Rev.*, D74:095010, 2006.

[28] B. C. Allanach, C. G. Lester, M. A. Parker, and B. R. Webber. Measuring sparticle masses in non-universal string inspired models at the lhc. *JHEP*, 09:004, 2000.

[29] L. Edelhäuser. LAMA model for O'Mega/WHIZARD. http://theorie.physik.uni-wuerzburg.de/∼ ledelhaeuser/lama/lama.html

[30] W. Kilian, T. Ohl, and J. Reuter. WHIZARD: Simulating Multi-Particle Processes at LHC and ILC. *hep-ph*/0708.4233, 2007.

[31] M. Moretti, T. Ohl, and J. Reuter. O'Mega: An optimizing matrix element generator. LC-TOOL-2001-040, *hep-ph*/0102195, 2001.

[32] P. Deuflhard. *Newton Methods for Nonlinear Problems*. Springer, 2004.

[33] B. C. Allanach et al. The Snowmass points and slopes: Benchmarks for SUSY searches. *Eur. Phys. J.*, C25:113–123, 2002.